Characterization of Metallic Nanowires by Combining Atomic Force Microscope (AFM) and Scanning Electron Microscope (SEM)

E. Celik* and E. Madenci**

*The University of Arizona, Tucson, AZ, 85721, USA, emrah@email.arizona.edu
**The University of Arizona, Tucson, AZ, 85721, USA madenci@email.arizona.edu

ABSTRACT

A new experimental method is introduced in order to characterize the mechanical properties of metallic nanowires. An accurate mechanical characterization of nanowires requires simultaneous imaging using scanning electron microscope (SEM) and mechanical testing with an atomic force microscope (AFM). In this study, an AFM is located inside an SEM chamber in order to establish the visibility of the nanowires. The tip of the AFM cantilever is utilized to bend and break the nanowires. Nanowire specimens are prepared by electroplating of metal ions into the nano-pores of the alumina membranes. Mechanical properties are extracted by using existing analytical formulations along with the experimental force versus bending displacement response. Preliminary results revealed that copper nanowires have unique mechanical properties compared to their bulk counterparts.

Keywords: atomic force microscope, nanomechanics, nanowire, scanning electron microscope

1 INTRODUCTION

Nanowires offer broad range of applications due to their unique properties especially in the fields of nano-electronics and computing technology. Mechanical characterization of nanowires is necessary in order to establish the feasibility of replacement of current electrical, mechanical and optical devices with nanowire integrated devices based on the reliability requirement. Although the characterization of electrical and optical properties of different types of nanowires has been studied extensively, mechanical characterization of nanowires still poses challenges to many existing testing and measurement techniques because of their small length scale. Manipulation and installation of individual nanowires in a test setup is rather challenging. Therefore, new mechanical characterization methods must be developed to quantify the mechanical properties of these nanostructures.

Existing nanowire mechanical characterization techniques in the literature can be grouped into three major categories; resonation of nanowires in an electron microscope, mechanical characterization via axial loading and bending of nanowires using atomic force microscope. The first technique involves the oscillation of nanowires inside an electron microscope by applying alternating voltage and examining the corresponding natural frequencies of nanowires [1-3]. Frequencies are then related to mechanical properties. Although this method is easy to perform, it is limited only to elastic properties of nanowires. Therefore, the yield and failure stresses, deformation and defect initiation mechanisms cannot be obtained. Mechanical characterization of nanowires has been performed by applying axial loading as well [4, 5]. In this method, nanowires or nanotubes are clamped in between two cantilevers and subjected to tension or compression loads in electron microscope. This technique requires significant amount of specimen preparation time and is not practical for testing of high number of nanowire specimens. The last group of mechanical characterization techniques involves bending of nanowires by using the tip of a commercially available AFM cantilever and this technique has been used successfully by several researchers [6-8]. However, commercial AFMs used in these studies are not capable of real time imaging of nanowires during testing. The correct alignment of nanowires according to AFM test probe poses a challenge due to the lack of nanowire visibility during testing. Also, deformation mechanism of nanowires cannot be investigated during testing. Therefore, there is a need for a new testing technique for mechanical characterization of nanowires that provides coexistence of two components of experimental analysis which are imaging and mechanical testing. A custom AFM placed in SEM for improved visibility can satisfy this requirement.

This study presents a new experimental test setup for bending test of nanowires involving a custom AFM and a SEM. The AFM is placed inside the SEM chamber; this high magnification imaging capability allows for correct alignment and placement of the specimens. Metallic nanowires with different sizes are fabricated using electroplating. Bending deformation measurements of nanowires concern different materials in different sizes.

2 MATERIALS AND METHODS

2.1 Specimen Preparation

Metallic nanowire specimens are prepared by electro-deposition of metal ions into nanopores of commercially available Whatman alumina membranes. Up to date, only copper nanowires have been grown in porous membranes with 200 nm pore diameter with this technique. A thin layer of metal is sputtered on one side of the alumina membrane as a contact layer onto which the nanowires grow. During electroplating, copper ions existing in electrolyte solution (0.5 M CuSO4) are deposited into the nanopores of the alumina membrane cathode. For the electroplating of copper, cathode voltage is set to -0.1 mV relative to the reference electrode and deposition duration is varied between 5 to 30 minutes which results in the deposition of nanowires in different lengths. After the nanowires are electroplated into the alumina membrane, the membrane is dissolved in 3M NaOH solution for 1 hour. Then, nanowires attached to the bottom metal layer are washed with distilled water and dissolved in toluene in ultrasonic bath. The vibration in the bath breaks the bonds between the nanowires and the thin metal layer and a homogenous distribution of nanowires in toluene is obtained. Nanowires dissolved in toluene solution are then spread over a silicon substrate. The substrate involves pre-etched trenches with the thickness range of 5 μm to 10 μm and the depth of 5 μm. After evaporation of toluene, some of the nanowires are suspended over the trenches and used for mechanical testing. The clamping of nanowires suspending on the trenches can be obtained by conformal deposition of a thin metal layer over the nanowires. The deposited thin metal film provides mechanical support for the mechanical testing of nanowires. After the nanowire specimens are prepared and clamped over the trenches of silicon substrate, they are tested using a custom AFM located inside SEM chamber.

2.2 Experimental Setup

The experimental setup combines the mechanical testing ability of AFM with imaging capability of SEM. The concept of locating a custom made AFM inside a SEM chamber is shown in Fig. 1.a. The detailed view of the custom AFM is given in Fig. 1.b. Main components of the setup are numbered in Fig. 1.b as follows:

1. AFM head
2. Micromotor
3. Laser diode
4. Photodiode
5. Piezoactuator
6. Mirrors
7. Manual control knobs

Electronic components are connected to a computer via National Instruments (NI) data acquisition boards. NI's Labview software is utilized in order to acquire photodiode signal and to control micromotor, laser diode and piezoactuator from outside the SEM chamber. Laser beam is used to monitor the deflection of the AFM cantilever during mechanical testing. In Fig. 1.b, the path of the laser beam from laser source to the photodetector is sketched. The laser beam is reflected by two mirrors before reaching the AFM cantilever. The third reflection of the laser occurs at the back of the cantilever and the reflected beam is directed to the final mirror before reaching to the quadrant photodiode.

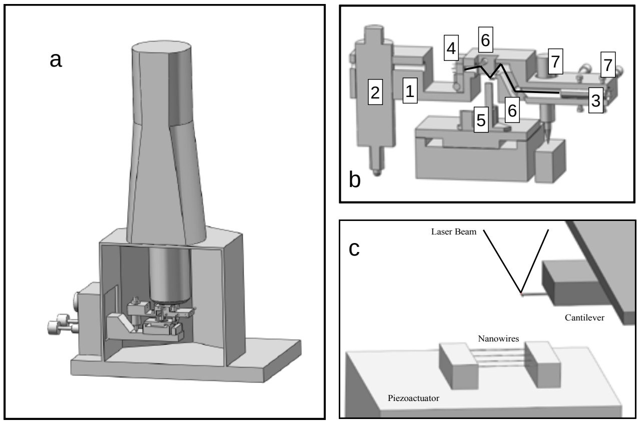

Figure 1: Experimental setup for mechanical testing of nanowires a) Location of AFM in SEM chamber, b) Custom AFM design, c) Detail of cantilever and nanowires

The tip of the AFM cantilever is positioned at the center of the nanowire located on the piezoactuator with respect to the nanowires. At this stage of the test, AFM cantilever and the nanowires are brought side by side without touching each other. After the vertical alignment is completed, the piezoactuator and the sample are moved towards the AFM tip, perpendicular to the nanowire axis establishing physical contact and causing the bending of the nanowires at the contact point by AFM tip. The lateral force acting between the nanowire and the AFM tip results in twisting of the cantilever and therefore changes the position of the laser beam on photodiode. The application of further load causes the nanowire to fracture and the laser beam goes back to original non-contact position on photodiode.

The change in the deflection of the AFM cantilever and the position of the laser beam on photodiode leads to change of the photodiode voltage which is converted into the data of force versus bending displacement of the nanowires in order to extract mechanical properties. The force exerted on nanowires can be obtained by multiplying the lateral deflection and the lateral stiffness of the AFM cantilever as given by Eq. (1).

$$F = k \times \delta_{cantilever} \qquad (1)$$

where k is lateral stiffness and $\delta_{cantilever}$ denotes the lateral deflection of the AFM cantilever. The lateral stiffness of the cantilever is obtained by using the dimensions and the shear modulus of the AFM cantilever. In order to obtain bending displacement of the nanowire at the contact point, deflection of the cantilever is subtracted from the total piezo displacement as follows;

$$\delta_{bending} = \delta_{piezo} - \delta_{cantilever} \qquad (2)$$

where $\delta_{bending}$, and δ_{piezo} represent bending displacement, and piezo displacement respectively. By using Eqs. (1) and (2), force versus bending displacement data can be obtained experimentally and these data are compared against the analytical formulations/models in order to extract mechanical properties of the nanowires.

In linear beam bending theory, the force acting on the mid-section of a double clamped beam is related to the bending displacement at the same location as follows;

$$F = \frac{192EI}{L^3}\delta_{bending} \qquad (3)$$

where *E, I, L* are Young's modulus, moment of inertia and length of the clamped portion of the beam. Therefore, the force is assumed to change linearly as a function of bending displacement. However, if the deformation of the nanowire beam is much larger than the diameter of the beam, the axial force acting on the beam leads to nonlinearity in force versus displacement variation. In this case, force can be defined by the approximate solution to the force/bending displacement expression according to [9].

$$F = \frac{192EI}{L^3}\delta_{bending}\left(1 + \frac{A}{24I}\delta^2{}_{bending}\right) \qquad (4)$$

The elastic limit of the nanowires can be estimated by using the linear and nonlinear analytical equations described above. The plastic zone is achieved after which the force versus bending displacement curve starts deviating from the predicted responses defined by Eqs. (3) and (4). The force at the deviation location is defined as the yielding force and at this point the yield stress can be described as follows according to [10].

$$\sigma_y = \frac{F_y L}{4\pi r^2 \delta_y} \qquad (5)$$

where r denotes the nanowire radius and F_y and σ_y are yielding force and yield stress respectively. δy is the bending displacement at the yield point. Similarly ultimate stress can be calculated by the equation described by [10].

$$\sigma_u = \frac{F_u L}{4\pi r^2 \delta_u} \qquad (6)$$

where and F_u , δ_u and σ_u are force, bending displacement and the ultimate stress at the failure point, respectively.

3 RESULTS

Bending displacement versus force relations obtained in four independent tests on copper nanowires are given in Fig. 2. According to these results, the force increases nonlinearly and decreases rapidly after the fracture of nanowires. The fracture points where the maximum force is achieved are marked by the arrows in the figure.

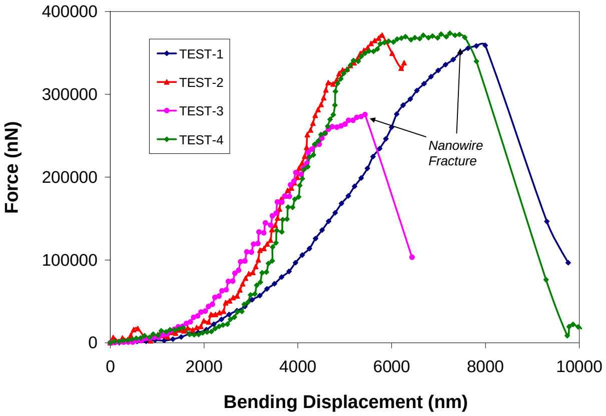

Figure 2: Force versus bending displacement variation.

In order to extract elastic modulus, force-bending displacement response of the nanowires obtained experimentally was compared against the predicted response described by Eq. (4). The elastic modulus values were obtained by matching the experimental and the predicted values. An example of the comparison between two data is given in Fig. 3. Force versus bending displacement data shows a remarkable agreement with the analytical model until the nanowire starts yielding, and the two responses deviate from each other.

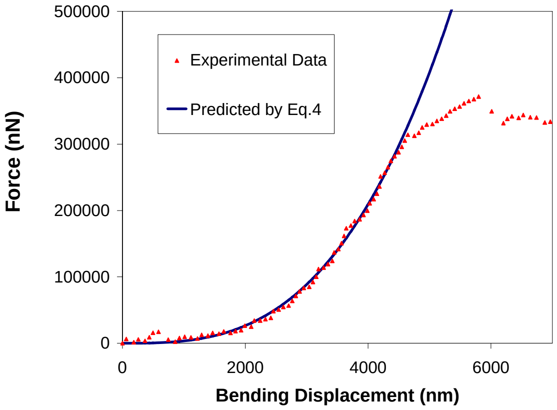

Figure 3: Comparison of experimental data and predictions.

The elastic modulus values for copper nanowires with 200 nm diameter were obtained between 2 to 3.5 GPa with an average of 2.7GPa. The elastic modulus of bulk copper is given as 110 GPa in the literature. The elastic moduli of the copper nanowires were observed to be significantly lower than that of the bulk material.

	Averaged Measured Value	Literature Value for Bulk Copper
Elastic Modulus (GPa)	2.7	110
Yield Stress (GPa)	2.3	0.05-0.3
Ultimate Stress (GPa)	2.8	0.23-0.38

Table 1: Averages of the mechanical properties obtained for 200 nm copper nanowires.

The yield stress values were calculated by using the Eq. (5) in four different tests and the results are given in Table 1. The yield stress of copper nanowires with 200 nm diameter was obtained between 1.01 and 3.09 GPA with an average value of 2.3 GPa. Average value of yield stress obtained in four tests is nearly an order of magnitude larger than the yield stress of the bulk copper which is given in literature within the range of 55-300 MPa.

The ultimate stress values of the nanowires were calculated by using Eq. (6) and the experimental data. The ultimate stress of copper nanowires was obtained between 2.32 and 3.31 GPA with the average value of 2.83 GPa (Table 1). The ultimate stress of bulk copper is given in the literature in the range of 230-380 MPa. The average value of ultimate stress obtained in this study is also an order of magnitude larger than the ultimate stress of bulk copper.

4 CONCLUSIONS

The preliminary results indicate that the elastic modulus (2.7 GPa) for copper nanowires with 200 nm diameter is significantly lower than that of the bulk material (110 GPa). This difference in elastic moduli is unexpected; therefore, it needs further investigation. Both the yield and ultimate strengths of the nanowires are an order of magnitude higher than those of the bulk copper. Higher mechanical strength can be explained due to reduced defect density at the nanoscale compared to the bulk scale [9]. High strength and durability of these nanowires in addition to their size advantages of copper nanowires will make them excellent candidates for many future applications.

REFERENCES

[1] Z. L. Wang, “Mechanical properties of nanowires and nanobelts”, Dekker Encyclopedia of Nanoscience and Nanotechnology, 1773-85, 2004.

[2] Y. Huang, X. Bai and Y. Zhang, “In situ mechanical properties of individual ZnO nanowires and the mass measurement of nanoparticles”, Journal of Physics: Condensed Matter, 18, 179-84, 2006.

[3] C. Q. Chen , Y. Shi, Y. S. Zhang, J. Zhu, and Y. J. Yan, “Size dependence of Young’s modulus in ZnO nanowires”, Physical Review Letters, 96, 075505, 2006.

[4] M. F. Yu, O. Lourie, M. J. Dyer, K. Moloni, T. F. Kelly, R. S. Ruoff, “Strength and Breaking Mechanism of Multiwalled Carbon Nanotubes Under Tensile Load”, Science, 287, 637-40, 2000.

[5] C. H. Lin, M. Chang, X. Li and J. R. Deka, “Measurement of Mechanical Properties of Boron Nanowire Using Nanomanipulation System”, Proceedings of the 35th International MATADOR Conference, 275-278, 2007.

[6] S. Paulo, J. Bokor, R. T. Howe, R. He, P. Yang, D. Gao, C. Carraro, and R. Maboudian, “Mechanical elasticity of single and double clamped silicon nanobeams fabricated by the vapor-liquid-solid method”, Applied Physics Letters, 87, 053111, 2005.

[7] H. Ni, X. Li, and H. Gao, “Elastic modulus of amorphous SiO2 nanowires”, Applied Physics Letters, 88, 043108, 2006.

[8] B. Wu, A. Heidelberg and J..J. Boland, “Mechanical properties of ultrahigh-strength gold nanowires”, Nature Materials, 4, 525-9, 2005.

[9] A. Heidelberg, L. T. Ngo, B. Wu, M. A. Phillips., S. Sharma, T. I. Kamins, J. E. Sader, and J. J. Boland, “A Generalized Description of the Elastic Properties of Nanowires”, Nano Letters, 6, 1101-6, 2006.

[10] D. Almecija, D. Blond, J. E. Sader, J. N. Coleman, and J. J. Boland, “Mechanical properties of individual electrospun polymer-nanotube composite nanofibers, Carbon, 47, 2253-8, 2008.